

Permutation Entropy for the Characterization of the Attractive Hamiltonian Mean-Field Model.

Melissa Fuentealba,^{*} Danilo M. Rivera,[†] and Roberto E. Navarro[‡]

Departamento de Física, Facultad de Ciencias Físicas y Matemáticas,

Universidad de Concepción, Concepción 4070386, Chile

(Dated: October 28, 2024)

Abstract

The Hamiltonian Mean-Field (HMF) model is a long-range interaction model that exhibits quasi-stationary states associated with a phase transition. Its quasi-stationary states with a lifetime diverging with the number of particles in the system. These states are characterized by homogeneous or non-homogeneous structures in phase-space. There exists a phase-transition between these states that have been traditionally characterized by their mean magnetization. However, the magnetization also exhibits fluctuations in time around its mean value, that can be an indicator of the kind of quasi-stationary state. Thus, we want to characterize the quasi-stationary states of the HMF model through the time-series of the magnetization and its fluctuations through a measure of information, i.e. the permutation entropy and the complexity-entropy plane. Permutation entropy is a measure for characterizing chaotic time series, especially in the presence of dynamic and observational noise, as it is computationally and conceptually simple. For non-homogeneous states, the permutation entropy shows that the HMF model tends towards order, while the magnetization fluctuations reveal reduced structures in time. On the contrary, homogeneous states tend to disorder and the structures of the magnetization fluctuations increase as the initial magnetization is larger. In all the study cases of this thesis, the HMF model is characterized by low entropy values but the highest possible complexity value. Thus, the HMF model can be described as a chaotic, deterministic and intermittent system. This aligns with previous studies of the model in the phase space. The results demonstrate that the HMF model can be understood and interpreted from the fluctuations of magnetization using permutation entropy and the complexity-entropy plane. Therefore, the measures used are powerful analytical tools for studying the information contained in the HMF model.

^{*} melifuatealba@udec.cl

I. INTRODUCTION

Systems with a large number of components interacting through long-range forces can become trapped in a quasi-stationary state (QSS), for periods of times increasing with the number of components, before reaching thermodynamic equilibrium [1]. For example, while studying the luminosity profiles of elliptical galaxies, Lynden-Bell [2] discovered that these systems were in an apparent stationary state different from the equilibrium state predicted by Chandrasekhar's theory (1942), and predicted relaxation times to equilibrium longer than the age of the universe. This phenomenon is observed not only in the dynamics of galaxies but also in various gravitational systems [3, 4] and plasmas [5]. In these systems, the dynamics are collective, making the statistical treatment extremely complex to apply due to the indeterminacy of the interaction distance.

The Hamiltonian Mean Field (HMF) model is one of the simplest models that shares characteristics with long-range interaction systems. It is analogous to the one-dimensional XY Heisenberg's model, where N spins can freely rotate in a plane under the action of an infinite range cosine potential [6]. One of its main characteristics is that it exhibits a non-collisional but violent relaxation process leading to out-of-equilibrium QSS [7]. In the QSS, the system displays inequivalence between its statistical ensembles, non-ergodicity, and its energy does not fulfill the properties of extensivity and additivity.

Typically, the QSSs of the HMF model have been studied by using a waterbag initial distribution for the spin's phase-space density, fully characterized by the total initial energy u_0 of the system and its average magnetization M_0 . In this case, there exists a non-equilibrium phase transition separating two types of QSS depending on M_0 and u_0 [8–10]: An homogeneous or demagnetized QSS, where the magnetization oscillates in time around an average $M_{QSS} = 0$, and traveling clusters probably due to trapping of resonant spins in phase-space [11, 12], and; A non-homogeneous or magnetized QSS, characterized by an average $M_{QSS} \neq 0$ and by a single non-traveling core-halo cluster in phase-space likely formed from a Landau damping-like mechanism of density waves [13]. Rivera and Navarro [14] suggested that other phase transitions may exist, as more than two cluster in phase space can be formed at high enough values of u_0 .

However, these QSS are not only characterized by the structures in the spin's phase-space

† danrivera@udec.cl

‡ roberto.navarro@udec.cl

and the average magnetization. Rivera and Navarro [14] noticed that the magnetization time series may present fluctuations with different amplitude and modulation characteristics, depending on the initial u_0 and M_0 , that may contain information of the type of QSS. Additionally, the HMF model is characterized by chaotic behavior and anomalous diffusive behavior of its particles over time [15–18]; it exhibits the formation of both ordered and disordered spatial structures [19, 20]; the formation of clusters can be considered as universal attractors [7, 13]; it is self-organized [10, 20]; it is robust in its quasi-stationary states (QSS) [6, 21, 22]; and it is compatible with the maximum entropy principle [23, 24]. These features can be utilized to characterize and understand the HMF model’s behavior as a complex system.

In this work, we characterize the fluctuations in the magnetization of the HMF model by using the permutation entropy [25]. The permutation entropy is one of various measures to characterize complex systems, which describes the dynamics of systems in terms of order and disorder, and can be used to evaluate the dispersion or randomness within an ordered series. It is a simple analytical measure, with an extremely rapid calculation speed, robust and invariant to linear and monotonic transformations, and useful if there is dynamic and observational noise [25]. A representation space based on this measure is the complexity-entropy plane [26], which differentiates between chaotic and stochastic systems, thus being able to understand the temporal dynamics of the system, differentiate between Gaussian and non-Gaussian processes, and among varying degrees of correlations.

Permutation entropy is a powerful tool to characterize the time series of magnetization fluctuations for varying initial conditions of the HMF model since it can analyze arbitrary time series, even in presence of dynamic and observational noise. Thus, in this work, we will study whether it is possible to characterize the QSS of the HMF model through the magnetization fluctuations, via the permutation entropy and the complexity-entropy plane.

II. NUMERICAL SIMULATIONS OF THE HAMILTONIAN MEAN-FIELD MODEL

Here, we use the attractive HMF model, which describes the gyromotion of N fully coupled spins freely rotating in a plane as described by the following Hamiltonian [8, 27]:

$$H = \frac{1}{2} \sum_{i=1}^N p_i^2 + \frac{1}{2N} \sum_{i,j=1}^N [1 - \cos(\theta_i - \theta_j)] , \quad (1)$$

where N is the total number of spins, θ_i is the angle of rotation of the i -th spin, and p_i its conjugate momentum. The second term in Eq. (1) is independent of the distance between spins, so it represents a potential of infinite range. The Hamilton's equations for each spin are then:

$$\dot{\theta}_i = p_i, \quad \dot{p}_i = -M_x \sin \theta_i + M_y \cos \theta_i, \quad (2)$$

where M_x and M_y are the components of the magnetization vector \vec{M} , given by

$$M_x = \frac{1}{N} \sum_{j=1}^N \cos \theta_j, \quad M_y = \frac{1}{N} \sum_{j=1}^N \sin \theta_j. \quad (3)$$

Note that the magnitude $M = \sqrt{M_x^2 + M_y^2}$ is a quantity normalized to the interval $0 \leq M \leq 1$. When $M = 0$, the orientation of all spins do not show a tendency towards a specific angle, so their θ -distribution is homogeneous. When $M = 1$, the spins are all oriented in the same direction.

Our simulations involve a large number of spins ($N = 10^6$), and the simulation time t is discretized into $\mathcal{N} = 2^{17} = 131\,072$ iteration steps with a temporal step $\Delta t = 0.01$. The equations of motion (2) are numerically solved through the classical second-order leap-frog method, which ensures that the total energy is conserved over time, with any possible oscillations remaining bounded.

The spins are initialized with random values of $|\theta_i| \leq \theta_0$ and $|p_i| \leq p_0$ following a waterbag distribution function. Thus, the initial conditions are characterized by either θ_0 and p_0 , or the initial total energy $u_0 = \frac{p_0^2}{6} + \frac{1}{2}(1 - M_0^2)$ and the initial magnetization $M_{x0} = M_0 = \frac{\sin(\theta_0)}{\theta_0}$ and $M_{y0} = 0$. Since $p_0^2 \geq 0$ must always be non-negative, then $u_0 < u_{\min}$ correspond to inaccessible states of the system, with $u_{\min} = (1 - M_0^2)/2$. In the rest of this text, we use u_0 and M_0 to characterize the initial conditions.

Due to phase-space symmetry, we expect $M_y(t) = 0$ at all times in the thermodynamic limit [7, 13]. However, due to randomness in particle simulations, we observe fluctuations in M_y that are nevertheless much smaller in magnitude than the fluctuations in M_x . Thus, in the following study we set $M_y = 0$ and neglect any fluctuations in it.

Figure 1 shows the time evolution of $M_x(t)$ for $M_0 = 0.8$ (or $\theta_0 \simeq 1.131$) and the two cases $u_0 = 0.5$ ($p_0 \simeq 1.39$) and $u_0 = 0.7$ ($p_0 \simeq 1.77$). Both cases quickly relax within the first 20 time steps from $M(0) = M_0$ to an average magnetization of $M_{\text{QSS}} = 0.63$ and $M_{\text{QSS}} = 0$ in

Figs. 1(a) and (b), respectively. This is a violent relaxation of the magnetization as described by Lynden-Bell [2]. Then, the system gets trapped in a QSS where the magnetization $M(t)$ fluctuates around the average M_{QSS} values. In Fig. 1(a), the fluctuations in $M(t)$ appear to be modulated, while in Fig. 1(b), these fluctuations are uniform but have higher intensity.

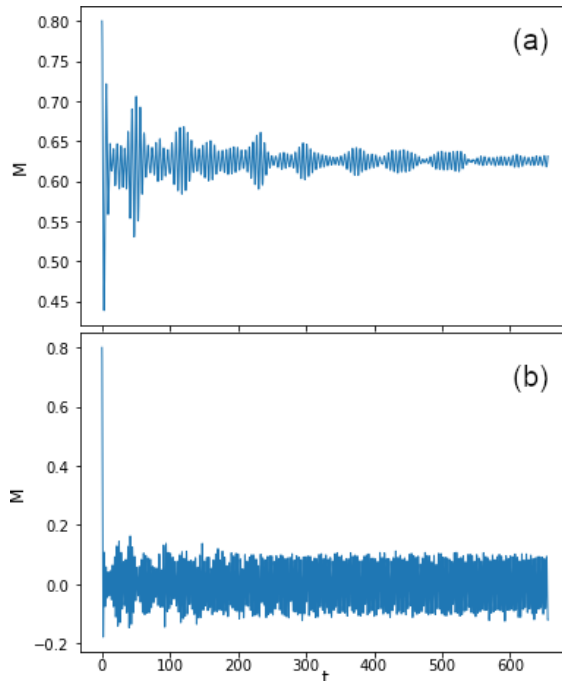


FIG. 1. Temporal evolution of the magnetization $M_x(t)$ starting with $M_0 = 0.8$ for (a) $u_0 = 0.500$, and (b) $u_0 = 0.700$.

Although not shown here, after $t = 100$, the spin's phase-space density associated to Fig. 1(a) is characterized by a persisting single cluster-like structure, with a core and halo limited to positions $|\theta| < 2$ and conjugate momentum $|p| < 1.5$ approximately, as reported by Pakter and Levin [13]. Conversely, Figure 1(b) is characterized by an almost filled and nearly homogeneous phase-space, with two clusters propagating in opposite directions.

To study only the region where the system is in a QSS, the time series were truncated from $t = 100$ (to remove the effects of the relaxation process on M) to $t \approx 755$, yielding $\mathcal{N} = 2^{16} = 65\,536$ data points per simulation. Figure 2 shows the average value M_{QSS} , calculated as the mean of the truncated time series of M during the QSS, as a function of u_0 for a fixed value of $M_0 = 0.8$. For energies $u_0 < 0.6$, $M_{\text{QSS}} > 0$ is a decreasing function of u_0 , representing a magnetized or inhomogeneous QSS. Around $u_0 = 0.6$, a phase transition occurs so that for $u_0 > 0.6$, $M_{\text{QSS}} \approx 0$ corresponding to nearly unmagnetized or

homogeneous states QSSs.

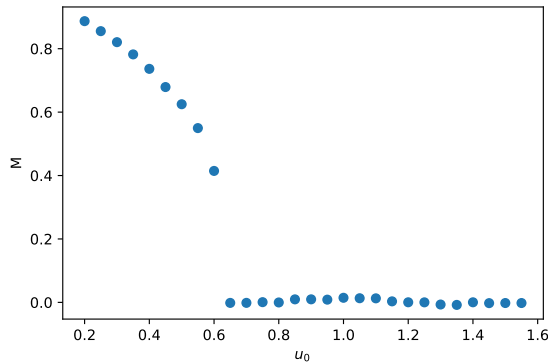


FIG. 2. Average magnetization M_{QSS} during the quasi-stationary state as a function of the initial energy u_0 for fixed $M_0 = 0.8$.

In this work, we will only focus on studying the time series of magnetization M in their QSS for different initial conditions u_0 and M_0 , without considering the information provided by the phase space.

III. PERMUTATION ENTROPY AND COMPLEXITY-ENTROPY PLANE

We briefly describe how to evaluate the permutation entropy for the fluctuations in the magnetization. Consider the time series $M_i = M(t = i\Delta t)$ with $0 \leq i \leq \mathcal{N}$ an integer representing the iteration time step. We subdivide this series into partitions of d elements as

$$W_p = \{M_p, M_{p+\tau}, M_{p+2\tau}, \dots, M_{p+(d-1)\tau}\}, \quad (4)$$

where $1 \leq p \leq n$ is the partition index, $n = \mathcal{N} - (d - 1)\tau$ is the total number of possibly overlapping time windows, $\tau \geq 1$ is the embedding delay denoting a temporal shift between windows, and $d > 1$ is the embedding window size [25].

Next, we construct n permutation sequences $\pi_p = \{r_0, r_1, \dots, r_{d-1}\}$ of the indices $0 \leq r_i \leq d - 1$ that would sort the elements of each partition W_p in ascending order. Then, we calculate the relative frequency in which any given sequence π is found among all the permutation sequences $\{\pi_p\}_{p=1\dots n}$, i.e.

$$\rho(\pi) = \frac{1}{n} \sum_{p=1}^n \delta(\pi, \pi_p), \quad (5)$$

where $\delta(\pi, \pi_p)$ is a delta-like function equal to 1 if $\pi = \pi_p$, and 0 otherwise.

Finally, the permutation entropy is the Shannon entropy of the probability distribution $\rho(\pi)$, which measures uncertainty or information content characterizing the probability distribution of ordinal patterns in a time series. Here, we use the normalized permutation entropy as [28]

$$H(\rho) = -\frac{1}{\log_2(d!)} \sum_{\pi} \rho(\pi) \log_2 \rho(\pi), \quad (6)$$

so that $0 \leq H \leq 1$, where $H \simeq 0$ suggests that there exists a predominant pattern, indicating more predictable data or a somewhat regular dynamics; and $H \simeq 1$ indicating a greater uncertainty or disorder in the time series.

On the other hand, the complexity-entropy plane was introduced by Rosso *et al.* [26] to distinguish between chaotic and stochastic time series. It is based on the statistical complexity measure proposed by López-Ruiz *et al.* [29], given by

$$C(\rho) = \frac{D(\rho, U)}{D_{\max}} H(\rho), \quad (7)$$

where $U = 1/d!$ is the uniform distribution for all possible sequences π , D_{\max} is a normalization constant, and $D(\rho, U)$ is the extensive Jensen-Shannon divergence [30] given by

$$D(\rho, U) = S\left(\frac{\rho + U}{2}\right) - \frac{1}{2}S(\rho) - \frac{1}{2}S(U), \quad (8)$$

where $S(\rho) = -\sum_{\pi} \rho(\pi) \log_2 \rho(\pi)$ is the unnormalized Shannon entropy.

The statistical complexity Eq. (7) is related to the interaction between the amount of information a system possesses and its imbalance, quantifying the degree of correlational structure in the series. For the numerical analysis of the permutation entropy and the statistical complexity, the open-source *ordpy* module [28] of the *Python* programming language was used. Recommended values for the window size are $d = 3$ to $d = 7$, and for the delay $\tau = 1$, as larger delays reduce the amount of available data for analysis. For the time series length, $\mathcal{N} \gg d!$ is often recommended, ensuring all ordinal patterns can be statistically observed [31]. Here, we set the embedding window as $d = 6$ and the embedding delay $\tau = 1$.

Figure 3 shows the permutation entropy H for the time series of the magnetization M , for all initial conditions M_0 and u_0 studied in this work. A cumulative vertical shift of 0.005 is added to each entropy curve for visual aid. Here, we considered nine equally spaced values of $0.1 \leq M_0 \leq 0.9$, where we excluded the cases $M_0 = 0$ because the dynamics is spatially homogeneous from the start (no gradients exist), and $M_0 = 1$ because all spins are aligned,

showing no change in the order parameter over time. For each value of M_0 (drawn with different colors in Fig. 3), we performed over 1000 simulations for initial energies in the range $u_{\min} < u_0 < 1.6$, where $u_{\min} = (1 - M_0^2)/2$ is the threshold of inaccessible states.

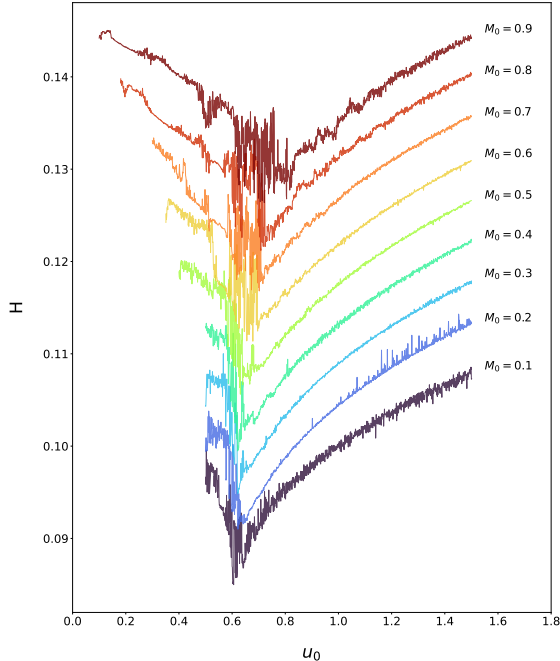


FIG. 3. Permutation entropy H of the magnetization time-series M during the QSS, as a function of the initial energy u_0 . Different values of the initial magnetization M_0 are drawn with different colors. A cumulative vertical shift of 0.005 is added to each entropy curve to focus on its trend.

For a fixed value of M_0 , all colored lines in Figure 3 show that the permutation entropy is monotonically decreasing with respect to u_0 , except for small fluctuations, up to approximately $u_0 \approx 0.6$. For higher energies, the permutation entropy increases almost monotonically. Additionally, as the value of M_0 increases, the entropy fluctuations near energies $0.6 < u_0 < 0.8$ also increase.

Although not shown here, calculations for the entropy of M or its fluctuations $\delta M = M - M_{\text{QSS}}$ result in exactly the same values of H . This is expected, as the entropy H is calculated by finding the indices that sort the time series, which is insensitive to a constant shifting M_{QSS} between M and δM . Thus, it is inferred that all the information about the QSS state can be fully extracted from the fluctuations of M without the need to calculate its average value M_{QSS} .

Therefore, for all values of M_0 , when H decreases for low energies up to $u_0 \sim 0.600$, it

indicates that the fluctuations of M tend towards order. This means that the modulation shown in Fig. 1(a) tends to decrease as u_0 increases and to show a well defined oscillation frequency. In contrast, when H increases for higher energies $u_0 > 0.6$, it indicates that fluctuations of M tend toward disorder, with a broadband frequency spectrum and with uniform amplitudes over time.

Near the global minimum of each curve in Fig. 3, we observe fluctuations in $H(u_0)$ whose amplitude and energy-range increase with M_0 . This is notorious starting from $M_0 = 0.6$ to $M_0 = 0.9$, where rough fluctuations appear around $0.6 \lesssim u_0 \lesssim 0.8$. This suggests that the trend towards order or disorder in δM in that energy range is not clear. Notice that a first order phase transitions separating the magnetized and demagnetized QSS has been reported for energies around $u_0 \simeq 0.6$ in the range $0 \leq M_0 \lesssim 0.6$. After $M_0 \gtrsim 0.6$, the order of the phase transition is unclear but it is strongly dependent on the initial conditions [32].

To calculate the statistical complexity Eq. (7), we first need to evaluate the Jensen-Shannon disequilibrium $Q(\rho, U) = D(\rho, U)/D_{\max}$ from Eq. (8). Figure 4 shows a plot of $Q(\rho, U)$ as a function of the initial energies u_0 for $M_0 = 0.8$. Calculations for other values of M_0 showed similar results. Here, Q increases almost monotonically for energies $u_0 \lesssim 0.6$ towards $Q = 1$, meaning that the distance between the probability distribution formed by the permutation patterns of the time series of M and the uniform distribution increases, and C is directly correlated to H . Thus, as H and C both decrease for increasing values of $u_0 \lesssim 0.6$, then the time series of M gradually tend to be ordered and to present fewer correlated structures as the energies increase. In this cases, the series of M values is an example of an ordered time series, as the reduction in fluctuations results in less variability and greater predictability in the magnetization values. Additionally, the decrease in the fluctuation amplitude shows that the relationship between the δM values is weak, so there are fewer trends or correlated structures in the time series.

For energies $u_0 \gtrsim 0.7$, Fig. 4 shows that Q , or the distance between ρ and U , decreases almost monotonically with u_0 . Still, both H and C increase as u_0 is increased, meaning that the fluctuations δM gradually tend to be disordered and to present a greater number of correlated structures as the energies increase.

The maximum disequilibrium is found near $u_0 \simeq 0.7$ with $Q \simeq 0.994$, but overall Q varies by only 3% in the whole energy range. This means that calculations of the statistical complexity Eq. (7) show similar trends between H and C , with H slightly greater than C

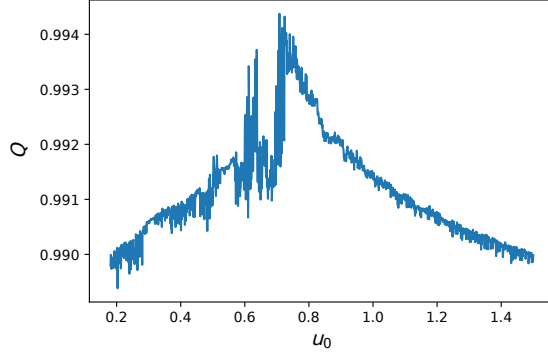


FIG. 4. Jensen-Shannon disequilibrium $Q(\rho, U) = D(\rho, U)/D_{\max}$, Eq. (8), as a function of the initial energies u_0 for $M_0 = 0.8$.

for all u_0 . As both H and C reach the minimum around that energy, which occurs near the reported phase-transition between magnetized and demagnetized QSS, then the phase-transition is characterized by the minimum possible degree of disorder, and a minimum of correlational trends in the fluctuations of M .

Figure 5 shows the complexity-entropy plane for simulations with initial $M_0 = 0.8$. This plot was divided into Fig. 5(a) for energies where the entropy is decreasing with u_0 , as shown in Fig. 3, and Fig. 5(b) for energies where the entropy increases with u_0 . Each colored point in the plane corresponds to a pair of entropy H and complexity C values calculated from the magnetization in the QSS for a given u_0 . The value of u_0 is indicated with the colors of the side bars. The black lines correspond to the minimum and maximum possible values of C [26, 28].

Figure 5 shows that both H and C are located in the lower-left zone of the entropy-complexity plane. Thus, fluctuations in M have characteristics of deterministic and chaotic systems of intermittent type. As u_0 is increased in Fig. 5(a), then fluctuations in M tend to be ordered and to present fewer correlated structures. This description is reversed as u_0 is increased in Fig. 5(b). In all cases, the calculated complexity C values are near the maximum possible complexity curve. This indicates that there are undoubtedly structures or distinguishable patterns in the values of the M time series.

Finally, we discuss whether the permutation entropy measure can provide information regarding the phase transition zone. Figure 6 shows a plot of the initial energies u_0 where the entropy H is minimum for a given value of M_0 , as extracted from Fig. 3. These points

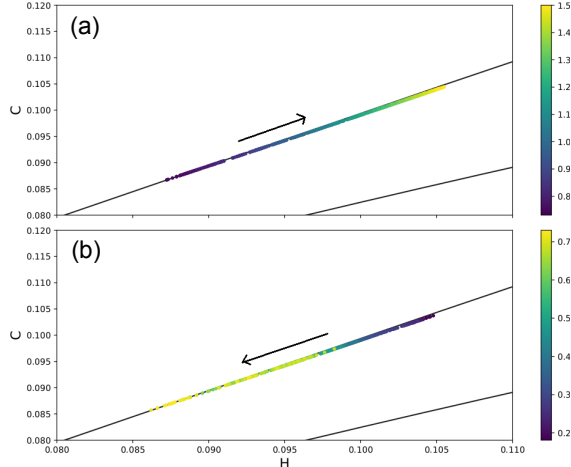


FIG. 5. Complexity-entropy plane associated to the magnetization time-series for the cases $M = 0.8$. The horizontal axis corresponds to permutation entropy H , and the vertical axis to the statistical complexity C . The color bar indicates the initial energy u_0 . The colorbar was divided into energies (a) $u_{\min} < u_0 < u_{\text{tran}}$ and (b) $u_{\text{tran}} < u_0$, where u_{\min} is the minimum accessible energy, and $u_{\text{tran}} \simeq 0.7$ is the energy where the entropy is minimum, as shown in Fig. 3. The arrows indicate the direction of increasing u_0 . The black lines are the minimum and maximum possible values of the statistical complexity.

correspond to the transition between order and disorder. Just for comparison, we include the virial curve $1 - 2u_0 = M_0 \cos \theta_0$, deduced by Benetti *et al.* [32], corresponding to initial conditions for which the magnetization is relatively invariant over time and its fluctuations are minimum. We also include the parameter region of inaccessible states $u_0 < (1 - M_0^2)/2$. The vertical bars indicate the range of energies where we observe wide amplitude fluctuations in the H trends of Fig. 3.

Below the blue line in Fig. 6 is characterized by states where the magnetization fluctuations tend to be ordered as u_0 increases. It is worth mentioning that the non-homogeneous QSS with average magnetization $M_{\text{QSS}} \neq 0$ are located below that curve. At least for $u_0 < 0.6$, this line coincides with the line of first order phase transition between magnetized and demagnetized QSS [32]. Thus, the permutation entropy and the characterization of order and disorder in the fluctuations of M alone can detect where the phase transition occurs.

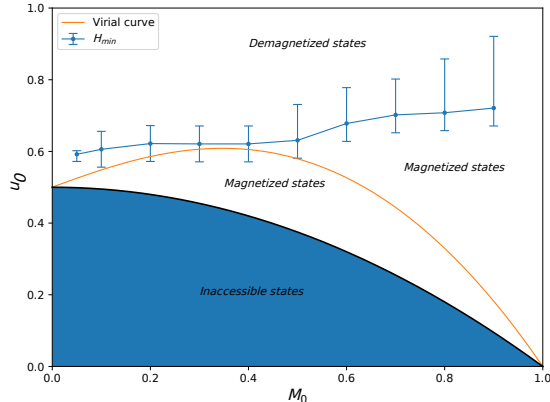


FIG. 6. Energies u_0 for which the permutation entropy H in Fig. 3 is minimum as a function of M_0 , represented as blue circled points. The vertical bars correspond to the energy ranges where H display wide fluctuations. The orange curve is the virial curve of the system, as indicated by Benetti *et al.* [32]. The blue area correspond to the u_0 and M_0 values that are inaccessible to the HMF simulations. Below the blue lines, the average magnetization in the QSS is characterized by $M_{\text{QSS}} > 0$. Above that line $M_{\text{QSS}} \simeq 0$.

IV. CONCLUSION

The Hamiltonian Mean-Field (HMF) model is a simple model used to describe systems with long-range interactions. This model presents magnetized $M_{\text{QSS}} = 0$ or demagnetized $M_{\text{QSS}} \neq 0$ quasi-stationary states (QSS), usually characterized by the average magnetization M_{QSS} during the QSS. There is a phase transition between these states, which has been previously studied in the literature by analyzing the distributions of positions and velocities of the model's particles. Our objective was to study the main phase transition present in the QSS only through the order parameter, defined as magnetization, because we were interested in how much information could be contained in this parameter and its fluctuations in time. Noticing that the HMF model has characteristics similar to those studied in complex systems, we studied the magnetization fluctuations by using an information measure given by the permutation entropy and the complexity-entropy plane.

By studying the magnetization M in the QSS of the model, we showed that the calculation of permutation entropy from M is insensitive to the average M_{QSS} . Thus, all the information about the QSS state can be extracted from the magnetization fluctuations alone.

Permutation entropy and the complexity-entropy plane showed that the fluctuations of

M tend towards order and fewer structures for initial energies $u_0 \lesssim 0.6$. For higher energies, the time series of magnetization fluctuations tend towards disorder and more structures. Additionally, the complexity-entropy plane shows that its permutation entropy H and statistical complexity C are located in the lower-left area of the plane, which is characteristic of intermittent deterministic chaotic systems.

Moreover, the minimum values of H coincide with the initial energies u_0 and magnetization M_0 where a reported phase transition between magnetized and demagnetized QSS occur [32]. Permutation entropy allowed us to characterize the QSS of the HMF model solely through the analysis of the time series of its order parameter or magnetization. This measure is a powerful tool, making it interesting to continue the study and, in the future, characterize the HMF model in its thermodynamic equilibrium.

-
- [1] V. Latora, A. Rapisarda, and C. Tsallis, Non-gaussian equilibrium in a long-range hamiltonian system, *Phys. Rev. E* **64**, 056134 (2001).
 - [2] D. Lynden-Bell, Statistical Mechanics of Violent Relaxation in Stellar Systems, *Monthly Notices of the Royal Astronomical Society* **136**, 101 (1967).
 - [3] T. Dauxois, V. Latora, A. Rapisarda, S. Ruffo, and A. Torcini, *The hamiltonian mean field model: from dynamics to statistical mechanics and back* (2002), [arXiv:cond-mat/0208456](https://arxiv.org/abs/cond-mat/0208456) [cond-mat.stat-mech].
 - [4] T. Padmanabhan, Statistical mechanics of gravitating systems, *Physics Reports* **188**, 285 (1990).
 - [5] Y. Levin, R. Pakter, and T. N. Teles, Collisionless relaxation in non-neutral plasmas, *Phys. Rev. Lett.* **100**, 040604 (2008).
 - [6] A. Pluchino, A. Rapisarda, and C. Tsallis, Nonergodicity and central-limit behavior for long-range hamiltonians, *Europhysics Letters* **80**, 26002 (2007).
 - [7] Y. Levin, R. Pakter, F. B. Rizzato, T. N. Teles, and F. P. Benetti, Nonequilibrium statistical mechanics of systems with long-range interactions, *Physics Reports* **535**, 1 (2014).
 - [8] A. Campa, T. Dauxois, and S. Ruffo, Statistical mechanics and dynamics of solvable models with long-range interactions, *Physics Reports* **480**, 57–159 (2009).
 - [9] A. Santini, G. Giachetti, and L. Casetti, Violent relaxation in the hamiltonian mean field

- model: Ii. non-equilibrium phase diagrams, *Journal of Statistical Mechanics: Theory and Experiment* **2022**, 013210 (2022).
- [10] R. Bachelard, C. Chandre, D. Fanelli, X. Leoncini, and S. Ruffo, Abundance of regular orbits and nonequilibrium phase transitions in the thermodynamic limit for long-range systems, *Phys. Rev. Lett.* **101**, 260603 (2008).
- [11] Y. Y. Yamaguchi, Construction of traveling clusters in the hamiltonian mean-field model by nonequilibrium statistical mechanics and bernstein-greene-kruskal waves, *Phys. Rev. E* **84**, 016211 (2011).
- [12] A. Antoniazzi, D. Fanelli, J. Barré, P.-H. Chavanis, T. Dauxois, and S. Ruffo, Maximum entropy principle explains quasistationary states in systems with long-range interactions: The example of the hamiltonian mean-field model, *Phys. Rev. E* **75**, 011112 (2007).
- [13] R. Pakter and Y. Levin, Core-halo distribution in the hamiltonian mean-field model, *Phys. Rev. Lett.* **106**, 200603 (2011).
- [14] D. M. Rivera and R. E. Navarro, Formation of multiple counter-propagating clusters in the attractive hamiltonian mean-field model (2022), [arXiv:2212.09608 \[nlin.PS\]](https://arxiv.org/abs/2212.09608).
- [15] V. Latora, A. Rapisarda, and S. Ruffo, Superdiffusion and out-of-equilibrium chaotic dynamics with many degrees of freedoms, *Phys. Rev. Lett.* **83**, 2104 (1999).
- [16] Y. Y. Yamaguchi, Relaxation and diffusion in a globally coupled hamiltonian system, *Phys. Rev. E* **68**, 066210 (2003).
- [17] A. Pluchino, V. Latora, and A. Rapisarda, Dynamical anomalies and the role of initial conditions in the hmf model, *Physica A: Statistical Mechanics and its Applications* **338**, 60–67 (2004).
- [18] F. Ginelli, K. A. Takeuchi, H. Chaté, A. Politi, and A. Torcini, Chaos in the hamiltonian mean-field model, *Phys. Rev. E* **84**, 066211 (2011).
- [19] T. Dauxois, P. Holdsworth, and S. Ruffo, Violation of ensemble equivalence in the antiferromagnetic mean-field xy model, *The European Physical Journal B* **16**, 659–667 (2000).
- [20] J. Barré, F. Bouchet, T. Dauxois, and S. Ruffo, Out-of-equilibrium states as statistical equilibria of an effective dynamics in a system with long-range interactions, *Phys. Rev. Lett.* **89**, 110601 (2002).
- [21] K. Jain, F. Bouchet, and D. Mukamel, Relaxation times of unstable states in systems with long range interactions, *Journal of Statistical Mechanics: Theory and Experiment* **2007**, P11008

- (2007).
- [22] F. Staniscia, P. H. Chavanis, G. De Ninno, and D. Fanelli, Out-of-equilibrium phase re-entrance(s) in long-range interacting systems, *Phys. Rev. E* **80**, 021138 (2009).
 - [23] A. Antoniazzi, D. Fanelli, S. Ruffo, and Y. Y. Yamaguchi, Nonequilibrium tricritical point in a system with long-range interactions, *Phys. Rev. Lett.* **99**, 040601 (2007).
 - [24] G. Martelloni, G. Martelloni, P. de Buyl, and D. Fanelli, Generalized maximum entropy approach to quasistationary states in long-range systems, *Phys. Rev. E* **93**, 022107 (2016).
 - [25] C. Bandt and B. Pompe, Permutation entropy: A natural complexity measure for time series, *Phys. Rev. Lett.* **88**, 174102 (2002).
 - [26] O. A. Rosso, H. A. Larrondo, M. T. Martin, A. Plastino, and M. A. Fuentes, Distinguishing noise from chaos, *Phys. Rev. Lett.* **99**, 154102 (2007).
 - [27] M. Antoni and S. Ruffo, Clustering and relaxation in hamiltonian long-range dynamics, *Phys. Rev. E* **52**, 2361 (1995).
 - [28] A. A. B. Pessa and H. V. Ribeiro, ordpy: A Python package for data analysis with permutation entropy and ordinal network methods, *Chaos: An Interdisciplinary Journal of Nonlinear Science* **31**, 063110 (2021).
 - [29] R. López-Ruiz, H. Mancini, and X. Calbet, A statistical measure of complexity, *Physics Letters A* **209**, 321 (1995).
 - [30] M. Martin, A. Plastino, and O. Rosso, Generalized statistical complexity measures: Geometrical and analytical properties, *Physica A: Statistical Mechanics and its Applications* **369**, 439 (2006).
 - [31] D. Cuesta-Frau, J. P. Murillo-Escobar, D. A. Orrego, and E. Delgado-Trejos, Embedded dimension and time series length. practical influence on permutation entropy and its applications, *Entropy* **21**, 385 (2019).
 - [32] F. P. d. C. Benetti, T. N. Teles, R. Pakter, and Y. Levin, Ergodicity breaking and parametric resonances in systems with long-range interactions, *Phys. Rev. Lett.* **108**, 140601 (2012).